Lawrence Berkeley National Laboratory
LBL Publications

Title

Robust Fe divalent state in one-unit-cell FeSe/SrTiO3 thin films

Permalink

https://escholarship.org/uc/item/9bh519sd

Journal

Physical Review B, 106(24)

ISSN

2469-9950

Authors

Shen, Jingdong

Jiang, Wenxiang

Zhu, Fengfeng

et al.

Publication Date

2022-12-01

DOI

10.1103/physrevb.106.245112

Peer reviewed

The robust Fe divalent state in one unit cell FeSe/SrTiO$_3$ thin film

Jingdong Shen,[1] Wenxiang Jiang,[2] Fengfeng Zhu,[3] Guan-yong Wang,[4] Huayao Li,[1] Gan Zhao,[1] Qian Li,[5] Wensheng Yan,[5] Wanli Yang,[6] Yi-De Chuang,[6] Jin-feng Jia,[7,8] Dong Qian,[7,8,*] L. Andrew Wray,[9,†] and Lin Miao[1,‡]

[1] *School of Physics, Southeast University, Nanjing 211189, China*
[2] *School of Physics and Astronomy, Shanghai Jiao Tong University, Shanghai 200240, China*
[3] *State Key Laboratory of Functional Materials for Informatics,*
Shanghai Institute of Microsystem and Information Technology,
Chinese Academy of Sciences, Shanghai 200050, China
[4] *Shenzhen Institute for Quantum Science and Engineering,*
Southern University of Science and Technology, Shenzhen 518055, China
[5] *National Synchrotron Radiation Laboratory, University of Science and Technology of China, Hefei, 230029, China*
[6] *Advanced Light Source, Lawrence Berkeley National Laboratory, Berkeley, California 94720, USA*
[7] *Key Laboratory of Artificial Structures and Quantum Control (Ministry of Education),*
Shenyang National Laboratory for Materials Science, School of Physics and Astronomy,
Shanghai Jiao Tong University, Shanghai 200240, China
[8] *Tsung-Dao Lee Institute, Shanghai Jiao Tong University, Shanghai 200240, China*
[9] *Department of Physics, New York University, New York, New York 10003, USA*
(Dated: November 8, 2022)

The orbital occupancy, as the origin of Hund's rule coupling, provides critical information in understanding the multi-orbital iron-based superconductors. The one unit cell (1UC) FeSe thin film on SrTiO$_3$ substrate with superconductive T_c above 60 K, has been reported with unique electronic structures as well as orbital occupancy. Here in this paper, we present the X-ray absorption spectroscopy (XAS) and resonant inelastic X-ray scattering (RIXS) study on the FeSe/STO thin films of different thicknesses. Together with the atomic multiplet simulation analysis, the FeSe/STO thin films (from 1UC to 10UC) are shown with the pure $3d6$ electronic configuration which is identical to the bulk FeSe. Moreover, 1UC FeSe/STO is found to be distinctively more persistent in hosting the $3d6$ configuration other than the thicker films under the oxidization process. The robustness of the $3d6$ in 1UC FeSe/STO is discussed as a result of charge transfer from the substrate, as well as a mechanism to maintain the high T_c superconductivity. At last, our research calls for a further high-resolution RIXS study on the pristine superconductive 1UC FeSe/STO thin film.

I. INTRODUCTION

The epitaxial one unit cell iron selenide on the SrTiO$_3$ (1UC FeSe/STO), receives broad interest due to its record-breaking high superconductivity transition temperature ($T_c \sim 65$K, or even to 100K) within the iron-based superconductors [1–4]. The T_c of 1UC FeSe/STO is about 8 times higher than its bulk crystal, raising the question about its differences with the bulk, and the core physical mechanism to enhance the superconductivity in the 1UC FeSe/STO [5]. Numerous experimental efforts have been made to unveil the mystery of superconductivity enhancement in the FeSe/STO interface. The surface spectroscopic methods (STM, ARPES, etc.,) have found the resonant phonon mode, associated with the charge transfer from the TiO$_2$-terminated STO might play the most critical roles [6–12]. These works incline to conclude that Cooper pairs in the 1UC FeSe/STO should be glued by phonons, similar to the conventional BCS-type superconductors. However, there is also theoretical and experimental evidence showing that 1UC FeSe/STO is possible with magnetic ground states, in the vicinity of the antiferromagnetic quantum criticality [13–17]. Such characteristics resemble the d-wave SC in cuprates. There is still an ongoing debate on the physical origin

of the enhanced SC in the 1UC FeSe/STO. The detection of magnetic many-body excitation or the resonant phonon excitation would be the smoking-gun evidence to solve the puzzle. While, the thin film is believed not capable of either neutron or X-ray scattering technique. Until last year (2021), it was reported that RIXS probed the gapped non-dispersive magnetic excitation in the 1UC FeSe/STO, which is never seen in the bulk FeSe[18, 19].However, their corresponding XAS characterization shows that the '1UC FeSe' thin film under study was with a clearly different d-orbital occupancy of Fe-ion than its counterpart in bulk FeSe [20]. This discrepancy reminds that previous experimental efforts focused on the low-energy quasiparticle dynamics but Fe-valence and associated d-orbital occupancy in the 1UC FeSe is not scrutinized. The Fe outer shell in iron-based SC is nearly half-filled($3d5$ or $3d6$), and manifest a prominent multi-band feature [21, 22]. The Hund's rule coupling which dominates the spin alignment, is a key correlation effect within the iron-based SC [23–25]. Thus, the valence state, essential to intra-atomic exchange, provides key information in understanding the d-orbital electronic correlation effect in the iron-based high-T_c superconductivity, especially the 1UC FeSe/STO [26].

In this paper, we present the systematic study on the FeSe/STO thin films with different thicknesses (from

1UC to 100UC) by using the XAS, and the RIXS. Together with atomic multiplet simulations, we clarified that the FeSe/STO films are all with low-spin $3d6$ configurations, rather than previously reported $3d5$-like states. Interestingly, the Fe-ion in 1UC FeSe/STO is highly persistent with $3d6$ configuration against oxidation, but thicker FeSe films trend to $3d5$ outer shell under the same oxidation process. Such behavior reaffirms the massive charge transfer effect on the interface between STO and 1UC FeSe is vital to the superconductivity. Our work proves that pristine 1UC FeSe thin film of $3d6$ state is a prerequisite for high-resolution RIXS experiments to detect the fundamental many-body excitations in this high T_c superconductor.

II. METHODS

All the FeSe/STO thin films are prepared by the epitaxial method (MBE), and amorphous selenium is capped to protect them against oxidation. The details of sample preparation are described in the Appendix A. All the FeSe/STO samples are transferred from the MBE chamber to the synchrotron endstation. Some of the samples immediately transferred to the experimental vacuum chamber for XAS experiment are defined as 'pristine', and other samples exposed to air for various days are defined as 'aged'. The se-capping layer is removed by annealing the sample up to 180°C inside the X-ray spectroscopy experiment chamber. Please note that the Se-capping layer of all samples was not removed until the XAS/RIXS measurement. Other details of XAS/RIXS experiments can be found in Appendix B. The probing depth of total electron yield (TEY) mode in XAS is well below ~3nm for the sub-KeV soft X-ray photons. Accordingly, the TEY signals are mostly generated from the outmost 1-2 unit cell of FeSe film for the L-edge XAS (hv~710eV) and the outmost 1 unit cell for the M-edge XAS (hv~55eV) [27, 28].

III. RESULTS AND DISCUSSION

First of all, to answer the question of whether the Fe-ion in 1UC FeSe has a different valence state or orbital occupancy than the bulk FeSe or not, the Fe L-edge ($2p$-$3d$) XAS are measured. Regardless of the thicknesses, one can see the freshly prepared FeSe samples of 1UC, 2UC, and 10UC thicknesses share the same Fe L-edge XAS (fig. 1a). These XAS curves are identical to the FeSe bulk, and very similar to the Fe-metal [20] because both FeSe and Fe-metal are with metallic ground states. The long-time air-exposed FeSe thin films clearly show a different XAS spectrum, even though they are protected with amorphous selenium during the exposure. The XAS of 170 days-aged 10UC FeSe bear splitting features in
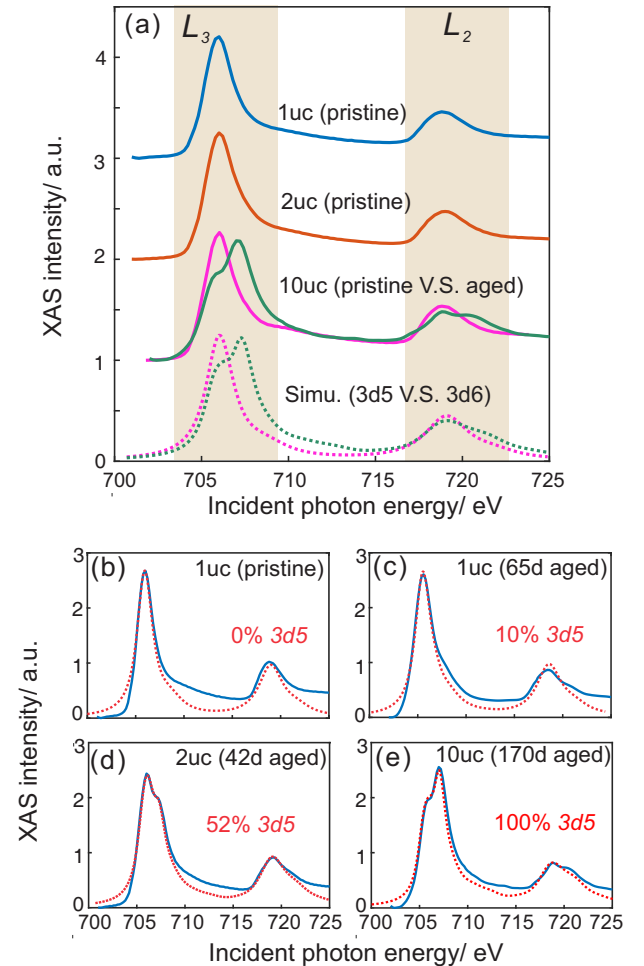

FIG. 1. **The L-edge XAS measurement of FeSe thin films and the corresponding fittings.** (a) The comparison of L-edge XAS curves of pristine 1UC (blue), 2UC (red) FeSe thin films, pristine (pink) and fully aged (green) 10UC FeSe thin films. The atomic multiplet simulated XAS curves of pure $3d5$ (Fe^{3+}, pink dashed) and $3d6$ (Fe^{2+}, green dashed) are present as reference. (b-e) The XAS curves (blue) of (b) pristine 1UC FeSe, (c) 65days aged 1UC FeSe, (d) 42days aged 2UC FeSe and (e) 170days aged 10UC FeSe fitted by the superpositions of simulated curves of $3d5$ simulations and $3d6$ simulations (red dashed). The ratio of $3d5$ simulated curves of fitting results is labeled.

both L_3 and L_2 peaks, and shifted the intensity of L_3 and L_2 peaks toward higher excitation energy. Those features of the split L_3 peak resemble the XAS of 1UC FeSe in Ref [18]. The split satellite peak on the L_3 edge with higher energy observed in Ref [18] was attributed to a hybridized orbital state from the STO substrate. However, it is missing in our experiment on the pristine FeSe thin films, but similar peaks with various intensities can be found in all the aged samples under air exposure. It is well-known that the amorphous Se film relaxes and degrades over time, so it is never perfect protection for a long time of exposure to air [29, 30]. The XAS of

FIG. 3. **The valence evolution as a function of air-exposure time.** (a) The $3d5$ portion extracted from the fitting of the pristine/aged FeSe thin films of different thicknesses. The data extracted from the M-edge XAS curves are marked with empty shapes and the L-edge XAS data are marked with filled shapes. The data of 1UC FeSe thin film is labeled in red color. The detailed XAS information included in this figure, as well as their fittings, are present in figure 1, figure 2, supplementary figure S2, and figure S3. (b) The low-spin $3d5$ and $3d6$ outer shell occupancy under the crystal field splitting of positive 10Dq.

plicit explanation is that Fe-ion in 1UC FeSe thin films are oxidized to trivalent, meanwhile, they receive extra electrons to compensate for the loss of charges. In other words, 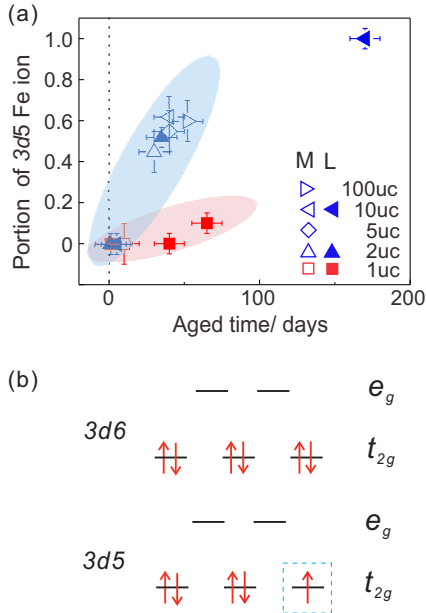there must be a charge source to revert the oxidized Fe-ions from the $3d5$ configuration to the $3d6$ configuration simultaneously. This charge source very much plays a role that is similar to the Lithium or the Natrium in the LiFeAs/NaFeAs, in which Fe-ion should be trivalent within the FeAs layer but manifest the divalency from XAS [32]. This mechanism can be directly associated with the profound charge transfer effect in the FeSe/STO interface. The doping of charges is found an essential avenue to give rise to an N-type Fermi surface. The STM, ARPES, and TEM work affirmed that such charge transfer effect is confined within the interfacial single UC FeSe, which explains why only 1UC FeSe thin film is more robust to keep the $3d6$ valence state.

Previous ARPES measurements and DFT calculations suggest that the electron-doping from the substrate is about 0.1 to 0.15 electrons per Fe-ion when it is of the $3d6$ valence state [10, 33], which is only about 20%-30% of charge transfer value (0.5 electrons per Fe-ion) extract from in Fig. 3a. One reason for this difference is that the $3d5$ valence state has a lower chemical potential than the $3d6$ valence state, resulting in extra potential difference and thus more electron doping from the substrate. The other reason that atomic multiplet simulation is based on the molecular orbital theory, is by assuming the materials are insulators. The itinerancy of the $3d6$ valence state in FeSe is omitted by the simulation, which magnifies the fitting errors. Accordingly, it is noteworthy that the deviation of the $3d5$ ratio extracted from the atomic multiplet simulation could be smaller than the real situation.

Whether a $3d5$ or $3d6$ outer shell will give rise to significantly different electronic and magnetic ground states. By consideration of the octahedral crystal field where the t_{2g} orbital is lower in energy, the $3d6$ would occupy all the t_{2g} orbitals but the $3d5$ will leave one electron unpaired (Fig. 3b). Although the crystal field of FeSe is in fact between an octahedral scenario and a tetrahedral scenario, and the e_g and t_{2g} orbital are possibly intertwined [22], the $3d5$ outer shell configuration would be more susceptible to the magnetic order. Moreover, a recent PES work suggests $3d5$ outer shell would also appear in the non-superconductive FeSe thin film when it is not sufficiently annealed after the sample growth [34], which also sets up the correspondence between the $3d6$ valence state and the superconductivity in 1UC FeSe/STO.

Due to the reason no appropriate experimental method to probe the many-body excitation in ultra-thin films, it has been a long debate about whether magnetic excitation exists in the parent phase of the FeSe thin film. RIXS is proven to be a high-efficiency scattering method to reveal the magnon in the single crystal of cuprates and iron-based superconductivity. RXIS study on the FeSe thin films was first reported in Ref. [18] and found it capable of detecting the possible magnetic excitation. Our discussion above indicates that the 1UC FeSe sample under study was possibly partially oxidized, and the excitations could be a result of the $3d5$ valence state, which is more susceptible to magnetism.

As well, we have performed the RIXS measurements on the pristine 10UC FeSe thin film (Fig. 4a-b) and the fully oxidized 10UC FeSe (Fig. 4c-d). Due to the limited energy resolution ($\sim$500meV) of our apparatus, the RIXS excitation peaks are very broad and we are not aimed at discovering fine peaks (Fig. 4b,d). The most pronounced discrepancy between the two sets of RIXS data is the elastic scattering signal (energy loss=0 eV). On the pristine 10UC FeSe, a candidate peak of elastic scattering arises only at the incident photon energy of 708 eV but is missing when the incident photon energy locates at the peak of Fe L_3-edge. For the oxidized 10UC FeSe, one can see that the elastic scattering peak is overwhelmingly high when the incident energy is tuned to Fe L_3-edge. Such an intensive elastic peak of Fe L-edge RIXS is not usually seen in other divalent iron-based superconductors [35, 36], but can be observed in the trivalent Fe (e.g., Fe_2O_3) [37] and the previously
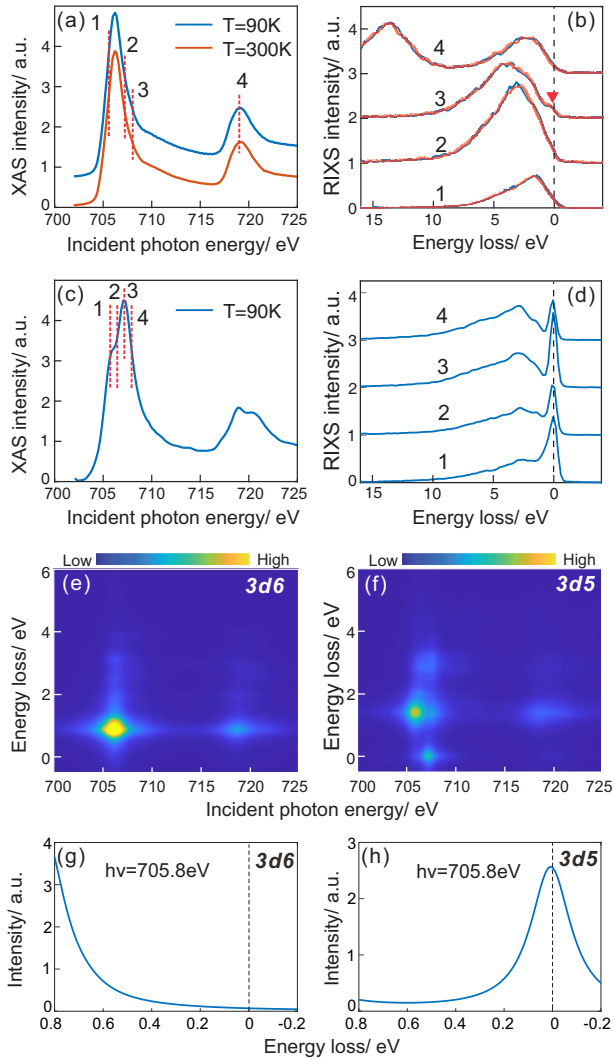
FIG. 4. **The RIXS measurement and corresponding RIXS simulations of the 10UC FeSe thin film.** (a) The L-edge XAS of pristine 10UC FeSe at T=90K (blue) and 300K (red). The incident photon energy for following RIXS measurement is marked by the vertical dashed lines. (b) The RIXS curves of four different incident photon energies (hv=705.6eV, 707.2eV, 708eV and 719eV) at T=90K (blue) and T=300K (red). (c) The L-edge XAS of 170 days aged 10UC FeSe at T=90K. The incident photon energy for following RIXS measurement is marked by the vertical dashed lines. (d)The RIXS curves of four different incident photon energies (hv=705.8eV, 706.4eV, 707eV and 707.6eV) at T=90K. (e-f) The simulated RIXS map with (e) $3d6$ outer shell and (f) $3d5$ outer shell. (g-h) The simulated RIXS curves with (g) $3d6$ outer shell and (h) $3d5$ outer shell with incident photon energy of hv=705.8eV.

reported RIXS of FeSe/STO (Fig. S14 in Ref [18]). To further justify our analysis of experiments, we performed the RIXS simulations. When the incident photon energy is tuned to L_3-edge, the simulated RIXS of the $3d6$ basis shows almost negligible elastic scattering signals (Fig. 4e,g), but the simulated RIXS of $3d5$ will give rise to a

considerable elastic peak (Fig. 4f,h). Accordingly, our RIXS experiments and simulations show high consistency that the elastic peak could be a good index to monitor the oxidization of FeSe thin films. That means the elastic peak could appear in the Fe L-edge RIXS with relative small intensity, and one needs to be very cautious if its intensity is overwhelmingly high.

IV. CONCLUSIONS

To conclude, our XAS&RIXS study on FeSe/STO thin films unambiguously reveals that FeSe thin films have the same $3d6$ outer shell of Fe-ion as the bulk FeSe. Meanwhile, the 1UC FeSe is surprisingly robust to host the $3d6$ valence state, and the charge transfer from the substrate is potentially the reason. We discussed that the charge transfer effect is uniquely essential because the $3d6$ orbital occupancy in 1UC FeSe is key to preserving its superconductivity. The previous study suggests that 1UC FeSe thin film is suitable for RIXS study to explore the possible magnetic excitations, but the present work indicates that the pristine FeSe thin film of divalence is necessary for probing the possible many-body excitations, as signatures for the electronic correlation.

Appendix A: Materials

The FeSe thin films were epitaxially grown on the Nb-doped (0.7%) SrTiO$_3$ substrate, following a standard procedure[2, 17]. All the films were post-annealed at ~500 °C for 1 hour after growth. The crystalline quality of FeSe thin films were monitored by the RHEED (see Fig. S1). The STM/STS is used to confirm the atomic-flat surface morphology and the superconductivity in the 1UC FeSe/STO (see Fig. S1). All the FeSe films are capped with amorphous selenium with a thickness of tens of nanometers before taking them out from the MBE chamber.

Appendix B: Experimental method

The soft X-ray absorption (Fe L-edge) spectroscopy and the related RIXS were performed in the iRIXS endstation at beamline 8 of Advanced Light Source and the Beamlines MCD-A and MCD-B (Soochow Beamline for Energy Materials) at NSRL. The integrated resolution of the RIXS is about 1000, which is about ∼700 meV at hv=700 eV. The RIXS measurements were with a fixed incidence angle of 30° and an exit angle of 60°. The UV X-ray absorption (Fe M-edge) spectroscopy was performed in the MERIXS endstation at BL4.0.1 of Advanced Light Source. The XAS was taken at temperature T=90K (Fe L-edge) and 10K (Fe M-edge) if no specific notes.

Appendix C: Atomic multiplet simulations

Atomic multiplet calculations were performed as in ref. [38] and [39], describing $2p^6\,3d^n \rightarrow 2p^5\,3d^{n+1}$ (L-edge) or $3p^6\,3d^n \rightarrow 3p^5\,3d^{n+1}$ (M-edge) X-ray absorption in the dipole approximation. Hartree-Fock parameters were obtained from the Cowan code [40], and full diagonalization of the multiplet Hamiltonian was performed using LAPACK drivers [41]. The crystal field splitting energy (10Dq) was set to 0.9 eV for the $3d6$ ground state. We have noticed that the 10Dq value was extracted as ∼0.5 eV in from the study on (Li,Fe)OHFeSe compound [42]. An extensive comparison (see supplementary fig. S5) show that the simulated XAS lineshapes are highly similar with 10Dq values varied from 0.4 eV to 1 eV. Meanwhile, the 10Dq value was set to 1.5 eV for $3d5$ ground state, which maybe due to the formation of Fe_2O_3 [43].

The atomic multiplet simulation parameters used in the M-edge are nearly identical to the L-edge, except the interaction coefficient ($F_{g\ p-d}$) between the $2p$-$3d$ orbital (L-edge) is renormalized to 66% of the $3p$-$3d$ orbital (M-edge). By fitting the M-edge XAS of FeSe and its oxidate, the relative energy shift between the $3d6$ simulated XAS curves and $3d5$ simulated XAS curves is a function of FeSe thickness. The relative shift energy is 0.6 eV (1UC FeSe), 3 eV (2UC, 5UC, and 10UC FeSe) and -0.4 eV (100UC).

---

* Electronic address: dqian@sjtu.edu.cn; Corresponding author

† Electronic address: lawray@nyu.edu; Corresponding author

‡ Electronic address: lmiao@seu.edu.cn; Corresponding author

[1] Q.-Y. Wang, Z. Li, W.-H. Zhang, Z.-C. Zhang, J.-S. Zhang, W. Li, H. Ding, Y.-B. Ou, P. Deng, K. Chang, *et al.*, Chin. Phys. Lett. **29**, 037402 (2012).

[2] W.-H. Zhang, Y. Sun, J.-S. Zhang, F.-S. Li, M.-H. Guo, Y.-F. Zhao, H.-M. Zhang, J.-P. Peng, Y. Xing, H.-C. Wang, *et al.*, Chin. Phys. Lett. **31**, 017401 (2014).

[3] J.-F. Ge, Z.-L. Liu, C. Liu, C.-L. Gao, D. Qian, Q.-K. Xue, Y. Liu, and J.-F. Jia, Nature Commun. **14**, 285 (2015).

[4] Z. Zhang, Y.-H. Wang, Q. Song, C. Liu, R. Peng, K. Moler, D. Feng, and Y. Wang, Sci. Bull. **60**, 1301 (2015).

[5] F.-C. Hsu, J.-Y. Luo, K.-W. Yeh, T.-K. Chen, T.-W. Huang, P. M. Wu, Y.-C. Lee, Y.-L. Huang, Y.-Y. Chu, D.-C. Yan, *et al.*, P. Natl. Acad. Sci. USA **105**, 14262 (2008).

[6] J. Lee, F. Schmitt, R. Moore, S. Johnston, Y.-T. Cui, W. Li, M. Yi, Z. Liu, M. Hashimoto, Y. Zhang, *et al.*, Nature **515**, 245 (2014).

[7] Y. C. Tian, W. H. Zhang, F. S. Li, Y. L. Wu, Q. Wu, F. Sun, G. Y. Zhou, L. Wang, X. Ma, Q.-K. Xue, and J. Zhao, Phys. Rev. Lett. **116**, 107001 (2016).

[8] C. Tang, C. Liu, G. Zhou, F. Li, H. Ding, Z. Li, D. Zhang, Z. Li, C. Song, S. Ji, K. He, L. Wang, X. Ma, and Q.-K. Xue, Phys. Rev. B **93**, 020507(R) (2016).

[9] D. Liu, W. Zhang, D. Mou, J. He, Y.-B. Ou, Q.-Y. Wang, Z. Li, L. Wang, L. Zhao, S. He, *et al.*, Nature Commun. **3**, 931 (2012).

[10] S. He, J. He, W. Zhang, L. Zhao, D. Liu, X. Liu, D. Mou, Y.-B. Ou, Q.-Y. Wang, Z. Li, *et al.*, Nature Mater. **12**, 605 (2013).

[11] S. Tan, Y. Zhang, M. Xia, Z. Ye, F. Chen, X. Xie, R. Peng, D. Xu, Q. Fan, H. Xu, *et al.*, Nature Mater. **12**, 634 (2013).

[12] H. Zhang, D. Zhang, X. Lu, C. Liu, G. Zhou, X. Ma, L. Wang, P. Jiang, Q.-K. Xue, and X. Bao, Nature Commun. **8**, 214 (2017).

[13] K. Liu, Z.-Y. Lu, and T. Xiang, Phys. Rev. B **85**, 235123 (2012).

[14] C. Tresca, F. Ricci, and G. Profeta, 2D Mater. **2**, 015001 (2014).

[15] H.-Y. Cao, S. Chen, H. Xiang, and X.-G. Gong, Phys. Rev. B **91**, 020504(R) (2015).

[16] Z. Wang, H. Zhang, D. Liu, C. Liu, C. Tang, C. Song, Y. Zhong, J. Peng, F. Li, C. Nie, *et al.*, Nature Mater. **15**, 968 (2016).

[17] Y. Zhou, L. Miao, P. Wang, F. F. Zhu, W. X. Jiang, S. W. Jiang, Y. Zhang, B. Lei, X. H. Chen, H. F. Ding, H. Zheng, W. T. Zhang, J.-f. Jia, D. Qian, and D. Wu, Phys. Rev. Lett. **120**, 097001 (2018).

[18] J. Pelliciari, S. Karakuzu, Q. Song, R. Arpaia, A. Nag, M. Rossi, J. Li, T. Yu, X. Chen, R. Peng, *et al.*, Nature Commun. **12**, 3122 (2021).

[19] M. C. Rahn, K. Kummer, N. B. Brookes, A. A. Haghighirad, K. Gilmore, and A. T. Boothroyd, Phys. Rev. B **99**, 014505 (2019).

[20] D. Telesca, Y. Nie, J. I. Budnick, B. O. Wells, and B. Sinkovic, Phys. Rev. B **85**, 214517 (2012).

[21] H. Hu, R. Yu, E. M. Nica, J.-X. Zhu, and Q. Si, Phys. Rev. B **98**, 220503(R) (2018).

[22] R. M. Fernandes and A. V. Chubukov, Rep. Prog. Phys. **80**, 014503 (2016).

[23] A. Kostin, P. O. Sprau, A. Kreisel, Y. X. Chong, A. E. Böhmer, P. C. Canfield, P. J. Hirschfeld, B. M. Andersen, and J. Davis, Nature Mater. **17**, 869 (2018).

[24] Z. Yin, K. Haule, and G. Kotliar, Nature Mater. **10**, 932 (2011).

[25] S. Mandal, P. Zhang, S. Ismail-Beigi, and K. Haule, Phys. Rev. Lett. **119**, 067004 (2017).

[26] A. Georges, L. d. Medici, and J. Mravlje, Annu. Rev. Condens. Matter Phys. **4**, 137 (2013).

[27] M. Abbate, J. Goedkoop, F. De Groot, M. Grioni, J. Fuggle, S. Hofmann, H. Petersen, and M. Sacchi, Surf Interface Anal **18**, 65 (1992).

[28] S. Schroeder, G. Moggridge, R. Ormerod, T. Rayment, and R. Lambert, Surf sci **324**, L371 (1995).

[29] W. C. Tan, G. Belev, K. Koughia, R. Johanson, S. K. O'Leary, and S. Kasap, J. Mater. Sci. Mater. Electron. **18**, 429 (2007).

[30] H. Lin, C. Cheng, K. Chen, C. Tseng, S. Huang, M. Chang, S. Tseng, M. Hong, and J. Kwo, APL Mater. **6**, 066108 (2018).

[31] J. Vura-Weis, C.-M. Jiang, C. Liu, H. Gao, J. M. Lucas, F. M. De Groot, P. Yang, A. P. Alivisatos, and S. R. Leone, J. Phys. Chem. Lett. **4**, 3667 (2013).

[32] E. Kurmaev, J. McLeod, N. Skorikov, L. Finkelstein, A. Moewes, Y. A. Izyumov, and S. Clarke, J. Phys.: Condens. Matter **21**, 345701 (2009).

[33] Y. Zhou and A. J. Millis, Phys. Rev. B **93**, 224506 (2016).

[34] H. Wang, A. Ghosh, C. Wang, S. Hsieh, Y. Shao, J. Chiou, C. Chen, C. Pao, J. Lee, Y. Liu, *et al.*, P. Natl. Acad. Sci. USA **116**, 22458 (2019).

[35] W. L. Yang, A. P. Sorini, C.-C. Chen, B. Moritz, W.-S. Lee, F. Vernay, P. Olalde-Velasco, J. D. Denlinger, B. Delley, J.-H. Chu, J. G. Analytis, I. R. Fisher, Z. A. Ren, J. Yang, W. Lu, Z. X. Zhao, J. van den Brink, Z. Hussain, Z.-X. Shen, and T. P. Devereaux, Phys. Rev. B **80**, 014508 (2009).

[36] X. Lu, W. Zhang, Y. Tseng, R. Liu, Z. Tao, E. Paris, P. Liu, T. Chen, V. N. Strocov, Y. Song, R. Yu, Q. Si, P. Dai, and T. Schmitt, Nature Physics **18**, 806 (2022).

[37] J. Miyawaki, S. Suga, H. Fujiwara, M. Urasaki, H. Ikeno, H. Niwa, H. Kiuchi, and Y. Harada, Phys. Rev. B **96**, 214420 (2017).

[38] L. A. Wray, J. Denlinger, S.-W. Huang, H. He, N. P. Butch, M. B. Maple, Z. Hussain, and Y.-D. Chuang, Phys. Rev. Lett. **114**, 236401 (2015).

[39] L. Miao, R. Basak, S. Ran, Y. Xu, E. Kotta, H. He, J. D. Denlinger, Y.-D. Chuang, Y. Zhao, Z. Xu, *et al.*, Nature Commun. **10**, 644 (2019).

[40] R. D. Cowan, "Robert d. cowan's atomic structure code," (1996), `https://www.tcd.ie/Physics/people/Cormac.McGuinness/Cowan/`.

[41] E. Anderson, Z. Bai, C. Bischof, L. S. Blackford, J. Demmel, J. Dongarra, J. Du Croz, A. Greenbaum, S. Hammarling, A. McKenney, *et al.*, *LAPACK Users' guide* (SIAM, 1999).

[42] Q. Xiao, W. Zhang, T. C. Asmara, D. Li, Q. Li, S. Zhang, Y. Tseng, X. Dong, Y. Wang, C.-C. Chen, *et al.*, arXiv preprint arXiv:2110.05361 (2021).

[43] N. Zhang, C. Liu, J.-L. Zhao, T. Lei, J.-O. Wang, H.-J. Qian, R. Wu, L. Yan, H.-Z. Guo, and K. Ibrahim, Chinese Physics B **25**, 097402 (2016).